文章编号:1001 - 2060(2016)11 - 0050 - 05

不同金属材料与海水温度对海水结垢影响的实验研究

杨大章[1],柳建华[2],吕　静[1],邱宇鑫[1]
(1. 上海理工大学 能源与动力工程学院,上海 200093; 2. 上海市动力工程多相流动与传热重点实验室,上海 200093)

摘　要: 针对海水换热结垢现象进行了实验研究。对比了镀锌铁片、黄铜、紫铜和不锈钢 4 种金属在海水中的结垢特征,以及 4 种金属表面结垢量的变化。实验结果显示,不同金属在海水中的污垢形貌及结垢量不同,镀锌铁片的结垢量最大,紫铜表面腐蚀较为严重,结垢量最小。对海水污垢进行了 XRD (X - Ray Diffraction) 和 EDX (Energy Dispersive X - Ray) 物相分析,结果显示,不同金属材料表面形成的海水污垢的物相组成不同,镀锌铁片表面的污垢成分主要是锌的腐蚀产物,而不锈钢表面的污垢成分主要为氢氧化镁。比较了镀锌铁片和黄铜在 80 ℃和 60 ℃海水中的结垢量变化,镀锌铁片污垢随着海水温度的上升而下降,而黄铜污垢随着海水温度的上升而上升。

关　键　词:海水污垢;金属材料;海水温度;影响因素;实验研究

中图分类号:P747　　**文献标识码**:A

DOI:10.16146/j.cnki.rndlgc.2016.11.009

引　言

海水的储量大,取得便利,是一种经济可行的换热媒介,但是海水在换热器金属表面极易发生结垢现象,常见的海水污垢主要有析晶污垢、腐蚀污垢和生物污垢[1-4]。海水中含有大量 Mg^{2+}、Ca^{2+} 等成垢离子,特别是 Mg^{2+},浓度高达 1 272 mg/L。当海水处于弱碱性条件下,易于生成析晶污垢。海水的导电性很强,电导率为 4.788 s/m,换热器中的合金在海水中极易发生电化学腐蚀,形成腐蚀污垢。海水换热污垢的生成,会导致换热效率的急剧下降和流动阻力的增加,从而导致换热器的冗余面积增加和输送能耗增加。根据英国工程数据库 ESDU 调查,在工业发达国家,换热器结垢造成的经济损失占到了 GDP 的 0.25%[1]。

本研究主要针对海水冷却水结垢过程及其影响因素进行了实验研究。通过对不同金属表面海水结垢的实验研究,研究了不同金属表面上海水结垢的物相组成和结垢规律。同时,实验研究了海水温度对结垢的影响,为海水换热器的设计和日常运行提供了可靠依据,有利于降低海水冷却水的结垢量、提高换热系数和降低运行能耗。

1　实验方法与装置

在海水冷却水系统中,输送海水介质的管道通常选用镀锌钢管或不锈钢管,主要的换热器材料通常选用紫铜和黄铜等金属。因此实验选用了镀锌铁片、不锈钢、紫铜、和黄铜这 4 种金属试片材料。实验使用的金属试片的具体尺寸如表 1 所示。

表 1　实验金属试片参数表

Tab. 1 Table of the parameters of metal test pieces

试片名称	尺寸/mm × mm	厚度/mm	表面自由能/mJ·m^{-2}
紫铜	100 × 65	0.2	187.56
黄铜	100 × 65	0.3	49.84
镀锌铁片	100 × 65	0.2	237.87
不锈钢	100 × 65	0.2	122.05

本实验使 4 种金属试片在海水环境中发生结垢现象,模拟了相应海水换热器和输送管道中的海水结垢现象。实验中将金属试片竖直悬挂在盛有 100 mL 海水的烧杯中,烧杯被放置在特定实验温度的

收稿日期:2015 - 11 - 27;　修订日期:2016 - 04 - 08
基金项目:上海市科委建设项目(13DZ2260900);上海大学生创新创业训练计划(SH2015118)
作者简介:杨大章(1986 -),男,浙江金华人,上海理工大学博士研究生.

恒温水箱中,水箱温度波动范围为 ±0.5 ℃。采用测量海水在金属表面的结垢量的方法是称重法。一旦金属试片被放置于海水溶液中,海水中的成垢离子在金属试片的表面异相成核,形成析晶污垢;金属表面在海水中发生腐蚀,形成腐蚀污垢。定时取出金属试片,经过烘干后进行称重,并将烧杯中的海水溶液进行替换。通过计算金属试片每次重量与初始值的差值即可得出金属试片表面的结垢量。

海水污垢的物相组成与海水中成垢离子的浓度有关。实验海水由海水晶配置,海水晶产地为江苏盐城。表 2 为海水的各离子浓度组成,其中成垢离子主要为 Mg^{2+},浓度达到了 1 272 mg/L。从表中可以得出,海水中 Ca^{2+} 的浓度并不高,海水结垢与一般江、河、湖和地下硬水结垢在物相组成上有较大的差别。

表 2　海水离子浓度

Tab. 2 Ion concentration of the seawater

成　分	Cl^-	Na^+	SO_4^{2-}	Mg^{2+}	Ca^{2+}	HCO_3^-	K^+	Al^{3+}
含量 mg/L	18 980	10 560	2 560	1 272	160	142	380	164

2　不同金属材料对海水污垢的影响

2.1　海水污垢形貌及结垢量实验结果

不同金属在海水中的结垢特性有很大不同。首先,不同的金属材料在海水中发生的电化学反应不同,造成海水污垢的成分和结垢量不同。其次,不同的金属材料具不同材料表面自由能和粗糙度,导致海水污垢晶体在金属表面的吸附和成核特性不同。通过实验研究对比了 4 种金属在海水中的结垢情况。图 1 为 4 种金属试片在 80 ℃海水中 100 h 后结垢的显微形貌图,从图中可以发现,镀锌铁片上的海水污垢非常明显,黄铜表面也存在大量白色晶体。而在紫铜表面,海水污垢的数量相对较少,在不锈钢表面只有零星污垢晶体存在,且表面呈现出褐色锈斑。

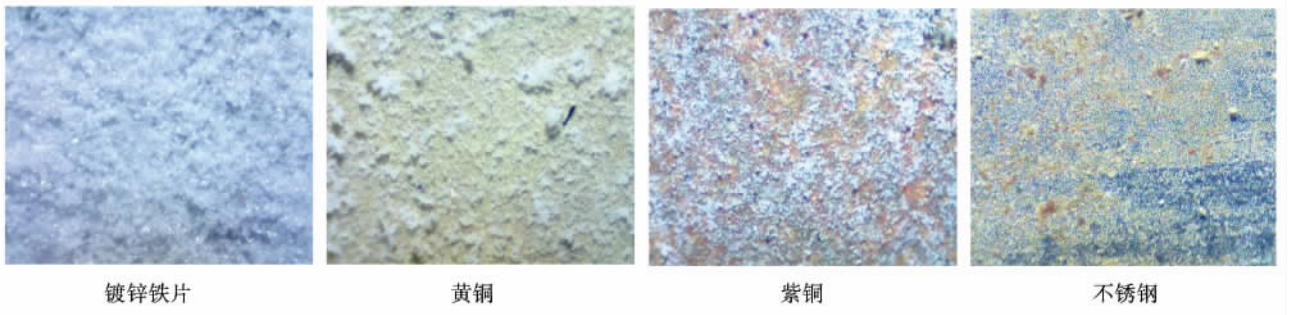

图 1　80 ℃海水中 4 种金属试片表面污垢形貌显微图(10×10 倍)

Fig. 1 Microscopic photos of the morphology of the fouls on the surface of four kinds of metal test piece in the seawater at 80 ℃

图 2 为 4 种金属在 80 ℃海水中 100 h 内的结垢量变化。从图中可知,海水结垢量最大的是镀锌铁片,其次是黄铜片,最少的是紫铜。镀锌铁片在海水中形成析晶垢十分快速,诱导期很短,在 0 ~ 50 h 内是结垢量持续增长期,在 50 h 以后,结垢量的变化趋于稳定且略有下降。这是因为,随着污垢厚度的不断增加,新生产的污垢不是吸附在金属表面,而是吸附在原有污垢的表面,吸附力大大降低,当污垢达到一定厚度,新生污垢容易发生剥离脱落。黄铜的诱导期很长,在 10 h 之前,黄铜的结垢现象很不明显,10 h 之后开始出现污垢。从表 1 金属试片表面自由能测量汇总表中可以看出,黄铜片的自由能

很小，只有 49.84 mJ/m^2，较小的自由能致使污垢晶体不容易在其表面附着，从而加长了诱导期。紫铜表面有轻微的结垢现象，但在海水中电化学腐蚀十分严重[15~16]，实验中悬挂紫铜的海水呈现蓝色，说明 Cu^{2+} 已经大量进入海水。紫铜成分为单质铜，铜与海水及空气发生化学反应，生成的二价铜离子在水中以水合离子 $[Cu(H_2O)_4]^{2+}$ 的形式存在。因为紫铜表面的铜单质不断地成为水合离子，紫铜片的质量逐渐减小，故实验数据反映的结垢量为负值。

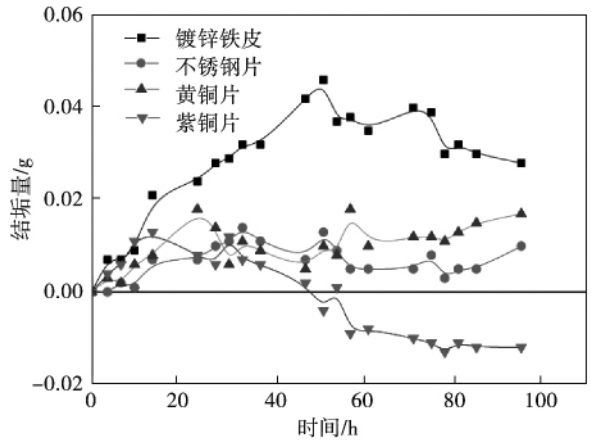

图 2 80 ℃条件下，4 种金属试片海水结垢变化

Fig. 2 Changes of the fouls on the surface of four kinds of metal test piece in the seawater at 80 ℃

2.2 镀锌铁片与不锈钢表面海水污垢物相分析

由于金属在海水中存在腐蚀现象，不同金属的表面海水污垢的组成也会存在差异。图 3 为镀锌铁片表面和不锈钢表面海水污垢的 XRD 图(X 射线衍射图)，从图中可以看出，两种污垢的衍射强度明显不同，如在镀锌铁片污垢 XRD 图中，第二波峰出现在 26°，而不锈钢污垢 XRD 图中第二波峰出现在 23°，这说明两种污垢的物相和晶体结构不同。表 3 为不锈钢和镀锌铁片表面污垢的 EDX 分析对比表，从表中可以看出，在不锈钢污垢中，含量最多的金属元素为 Mg，且存在 Ni 和 Fe 等金属元素。而在镀锌铁片污垢中，含量最多的金属元素为 Zn，其次为 Mg。这是因为 Zn 的化学性质较活泼，在海水中极易发生腐蚀，且在碱性环境中易产生 $Zn(OH)_2$ 沉淀。

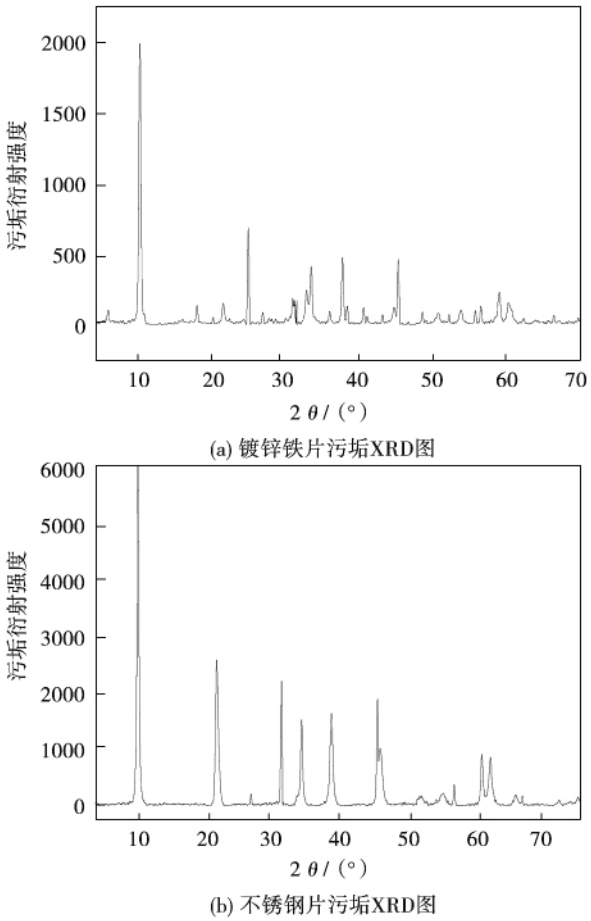

图 3 海水污垢 X 射线衍射图

Fig. 3 X-ray diffraction photo of the fouls in the seawater

3 海水温度对结垢的影响

在海水结垢环境中，海水温度直接影响了污垢结晶和腐蚀反应自由能，也决定了成垢离子的平均动能和碰撞概率，从而对结垢速率和结垢量造成影响。从上文中已知，不同金属表面在海水中产生污垢成分不同，因此不同金属受海水温度的影响也有不同。在能源和动力领域的海水冷却系统中，海水往往用于冷却水蒸气，因此海水的换热温度很高，在船舶柴油机中冷却水温度是 80 ℃左右[17]，在核发电站中乏燃料的冷却水池最高温度也为 80 ℃[18]。因此实验选用 80 ℃和 60 ℃的海水进行实验，以反映海水温度对结垢的影响。图 4 和图 5 分别为镀锌铁片和黄铜在 80 ℃和 60 ℃海水中结垢量的变

化曲线。

表 3　不锈钢与镀锌铁片表面海水污垢元素组成对比表

Tab. 3 Table of the contrast of the element composition of the fouls on the surface of stainless steel and galvanized iron sheets in the seawater

元素	不锈钢表面海水污垢/%		镀锌铁片表面海水污垢/%	
	质量百分比	原子百分数	质量百分比	原子百分数
C	5.24	9.07	3.71	8.02
O	38.3	49.75	29.88	48.52
Si	0.29	0.22	–	–
S	0.77	0.5	4.37	3.54
Cl	13.65	8	15.01	10.99
Mg	24.45	20.9	13.49	14.41
Al	9.6	7.39	–	–
Ca	–	–	4.77	3.09
Fe	0.82	0.3	–	–
Ni	1.82	0.64	–	–
Zn	–	–	28.77	11.43

对于镀锌铁片表面的污垢,从图 4 中可以看出,60 ℃海水的结垢量渐近值明显要大于 80 ℃海水的结垢量渐近值。在镀锌铁片发生结垢的前 20 h,60 ℃和 80 ℃海水的结垢量区别不大,而在 20 h 后,60 ℃海水中污垢增长率要明显大于 80 ℃海水中的污垢增长速率,60 ℃海水的污垢量也显著大于 80 ℃海水的结垢量。简而言之,在镀锌铁片表面,海水温度的升高,虽然增加了成垢离子的扩散速率和反应速率,但是镀锌铁片表面的污垢量反而下降了。

在黄铜表面的海水污垢受温度的影响与镀锌铁片表面正好相反。从图 5 中可以看出,在 80 ℃海水中黄铜表面结垢量要大于在 60 ℃的海水的情况。这种差别主要是由镀锌铁片和黄铜表面的污垢物相组成引起的。黄铜表面的污垢成分主要是由海水中 Mg^{2+} 形成的氢氧化镁。氢氧化镁是一种反向溶解度的物质,溶解度随着温度的上升而下降,从而导致结垢量增加。而镀锌铁片的污垢晶体主要是锌的腐蚀产物,即锌盐和氢氧化锌等。这些晶体微溶于水,溶解度随着温度的升高而上升,较高的海水温度将导致结垢量的减少。

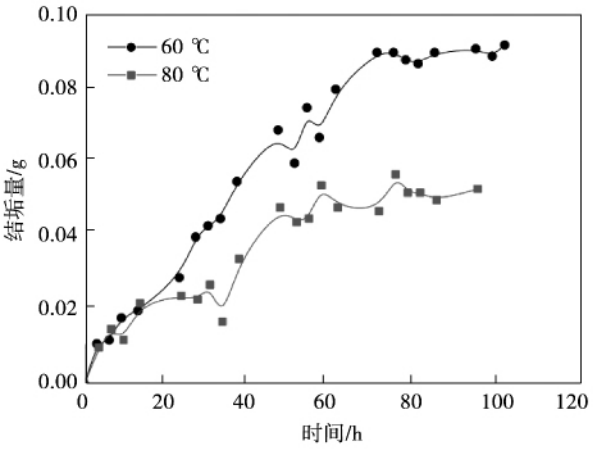

图 4　镀锌铁片表面海水结垢量变化

Fig. 4 Changes of the amount of fouls on the surface of a galvanized iron sheet in the seawater

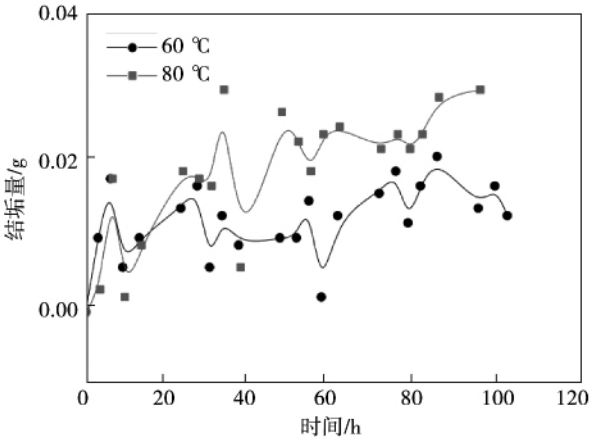

图 5　黄铜表面海水结垢量变化

Fig. 5 Changes of the amount of fouls on the surface of a brass sheet in the seawater

4　结　论

对海水换热器的结垢问题进行了实验研究,对比了镀锌铁片、不锈钢、黄铜和紫铜在海水中的结垢情况。对海水污垢进行了 XRD 和 EDX 物相分析,结果显示海水污垢由海水中的成垢离子和金属腐蚀产物组成。不锈钢表面腐蚀污垢主要为氢氧化镁;镀锌铁片表面海水污垢主要是锌的腐蚀产物;黄铜在海水中污垢量较少;紫铜在海水中存在腐蚀和溶解的现象。另外,实验研究了在 80 ℃和 60 ℃的海

水中金属表面结垢量的变化。实验结果显示，镀锌铁片海水结垢量随着海水温度的上升而下降，而黄铜海水结垢量随着海水温度的上升而上升。

参考文献:

[1] Engineering Sciences Data Unit. Guide to industrial water conservation, part 1: Water reuse in single contaminant systems [R]. ESDU Item No. 00020, ESDU International Plc., London, UK, 2000.

[2] 毕海洋. 污水源热泵系统取水换热过程流化除垢与强化换热方法 [D]. 大连理工大学, 2007.
BI Hai-yang. Foul fluidized-removing and enhanced heat exchange method for the water intaking and heat exchange process of a sewage water source heat pump system [D]. Dalian: Dalian University of Science and Technology, 2007.

[3] Pugh S J. Fouling during the use of seawater as coolant—the development of a user guide [J]. Heat Transfer Engineering, 2005, 26(1): 35 – 43.

[4] 郭 琨. 海洋手册 [M]. 北京: 海洋出版社, 1984.
GUO Kun. Marine handbook [M]. Beijing: Ocean Press, 1984.

[5] 钟云泰. 珠海发电厂循环冷却水系统海生物污染研究 [J]. 东北电力技术, 2004, 25(7): 12 – 16.
ZHONG Yun-tai. Resesarch of the ocean-borne biological pollution in the circulating cooling water system of Zhuhai Power Plant [J], Northeast Electric Power Technology, 2004, 25(7): 12 – 16.

[6] 汪长春, 王成铭, 郑文远. 大亚湾和岭澳核电站海水冷却系统的腐蚀与控制 [J]. 电力安全技术, 2009, 11(2): 17 – 20.
WANG Chang-chun, WANG Cheng-ming, ZHEN Wen-yuan. Corrosion and control of the seawater cooling system of Daya Bay and Ling Ao Nuclear Power Station [J]. Electric Power Safety Technology, 2009, 11(2): 17 – 20.

[7] 王 冶. 船用换热器流动与传热的三维流场数值模拟研究 [D]. 上海: 上海交通大学, 2013.
WANG Ye. Numerical simulation and study of the 3d flow field of the flow and heat transfer in a marine heat exchanger [D]. Shanghai: Shanghai Jiaotong University, 2013.

[8] 王 冶, 徐筱欣. 船用换热器三维流场数值模拟 [J]. 中国舰船研究, 2013, 8(4): 79 – 85.
WANG Ye, XU Xiao-xin. Numerical simulation of the 3d flow field in a marine heat exchanger [J]. China Warship Research, 2013, 8(4): 79 – 85.

[9] 张 莉, 胡松涛. 海水作为热泵系统冷热源的研究 [J]. 建筑热能通风空调, 25(3): 34 – 38.
ZHANG Li, HU Song-tao. Study of a heat pump system with seawater serving as the cooling and heat source [J]. Thermal Energy, Ventilation and Air Conditioning in Buildings, 25(3): 34 – 38.

[10] Satoru O. A heat pump system with a latent heat storage utilizing seawater installed in an aquarium [J]. Energy and Buildings, 2006, 38(2): 121 – 128.

[11] 许 凯, 王金昌, 严易明, 等. 开架式海水气化器换热管内流场和传热数值模拟研究, 石油化工设备, 40(s2) 2011: 7 – 10.
XU Kai, WANG Jin-cang, YAN Yi-ming, et al. Numerical simulation of fluid flow and heat transfer in heat tube of open shelf water gasification exchanger [J]. Petroleum and Chemical Engineering Equipment, 40(s2) 2011: 7 – 10.

[12] 杨文刚, 陈 杰, 浦 晖. 海水换热器在大型 LNG 工厂的应用 [J]. 制冷技术, 33(2): 45 – 47.
YANG Wen-gang, CHEN Jie, PU Hui. Applications of the seawater heat exchangers in large-scale LNG plants [J]. Refrigeration Technology, 33(2): 45 – 47.

[13] 俞 洁. 用于海水源热泵系统的抛管式换热器优化研究 [D]. 天津: 天津大学, 2012.
YU Jie. Study of the optimization of casted heat exchangers for use in seawater source heat pump systems [D]. Tianjing: Tianjing University, 2012.

[14] Izadi M, Aidun D K, Marzocca P, et al. Integrated experimental investigation of seawater composite fouling effect on the 90/10 Cu/Ni tube [J]. Applied Thermal Engineering, 2011, 31(14): 2464 – 2473.

[15] Sandberg J, Wallinder I O, Leygraf C, et al. Corrosion-induced copper runoff from naturally and pre-patinated copper in a marine environment [J]. Corrosion Science, 2006, 48(12): 4316 – 4338.

[16] Kear G, Barker B D, Walsh F C. Electrochemical corrosion of unalloyed copper in chloride media-a critical review [J]. Corrosion Science, 2004, 46(1): 109 – 135.

[17] 高洪涛, 鞠晓群, 毛宝龙. 以船舶柴油机冷却水余热为热源的 TFE/TEGDME 吸收式制冰系统 [J]. 工程热物理学报, 2013, 34(7): 1204 – 1208.
GAO Hong-Tao, JU Xiao-qun, MAO Bao-long. TFE/TEGDME absorption type ice-making system with the waste heat from the cooling water in a marine diesel engine serving as the heat source [J]. Journal of Engineering Thermophysics, 2013, 34(7): 1204 – 1208.

[18] 叶水祥. 乏燃料水池内流动与传热数值分析 [D]. 哈尔滨: 哈尔滨工程大学, 2012.
YE Shui-xiang. Numerical analysis of the flow and heat transfer in a waste fuel water pool [D]. Harbin: Harbin Engineering University, 2012.

(刘 瑶 编辑)

porting vector machine, supporting vector regression machine

撞击预燃室煤粉燃烧器气固两相流特性研究 = Gas-Solid Two-Phase Flow Characteristics of the Pulverized Coal Burner with Impinging Pre-combustion Chamber [刊,汉] /WANG Shuai, FAN Bao-guo, LIU Hai-yu, JIN Yan(College of Electrical and Power Engineering, Taiyuan University of Technology, Shanxi Taiyuan 030024)//Journal of Engineering for Thermal Energy & Power. -2016, 31(11). -43 ~49

The gas-solid two-phase flow characteristics of the pulverized coal burner with impinging pre-combustion chamber were numerically (by Fluent) and experimentally studied. The flow field, fuel concentration and particle trajectories of the burner were examined under different secondary air angles. It is concluded that there is open air in the burner when the secondary air angle is(30°,45°). The tangential and axial angles of the secondary air have an important influence on the air flow spreading angle, vortex intensity and flow jet length. The flow field and particle trajectories become more reasonable when the secondary air angle is (5°,20°). **Key words:** pulverized coal burner; gas-solid two-phase flow; experimental research; numerical simulation

不同金属材料与海水温度对海水结垢影响的实验研究 = Experimental Study of the Influence of Various Metal Materials and Seawater Temperature on Seawater-caused Fouling [刊,汉] /YANG Da-zhang, LV Jing, QIU Yu-xin (Shanghai University of Science and Technology, Shanghai, China, Post Code: 200093), LIU Jian-hua (Shanghai City Key Laboratory on Multi-phase Flow and Heat Transfer in Power Engineering, Shanghai, China, Post Code: 200093)//Journal of Engineering for Thermal Energy & Power. -2016, 31(11). -50 ~54

Experimentally studied were the fouling phenomena existing in the heat exchange process of seawater and compared were the fouling characteristics of four kinds of metal in seawater, i. e. a galvanized iron plate, brass, copper and stainless steel material and changes of the amount of fouls on the surface of four kinds of metal. The test results show that the fouling morphology and amount of fouls formed in seawater are varied in metals, the galvanized iron plate has the largest amount of fouls and the copper materials have the comparatively serious corrosion but the smallest amount of fouls on the surface. A XRD (X-Ray Diffraction) and EDX (Energy Dispersive X-Ray) phase analysis was performed of the seawater-caused fouls. It has been found that the phase composition of the seawater-caused fouls formed on the surface of various metal materials is varied and the constituents of the seawater-caused fouls on the surface of a galvanized iron plate are mainly the products produced in the process of erosion and corrosion of zinc, however, those on the surface of stainless steel materials are mainly magnesia hydroxide. Changes of the amount of fouls formed on the surface of a galvanized iron plate and a brass material in seawater at 80 ℃ and 60 ℃ were compared. It has been found that the amount of fouls formed on the surface of the galvanized iron plate will increase with a decrease of the seawater temperature, however, that formed on the surface of brass materials

will increase with an increase of the seawater temperature. **Key words:** seawater-caused foul, metal material, seawater temperature, influencing factor, experimental study

基于窄带模型的新灰气体加权和模型关联式 = New Weighted Sum of Grey Gases Model Correlation Formula Based on Statistical Narrow Band Model [刊,汉] /NIE Yu-hong (School of Marine Engineering, Guangzhou Maritime University, Guangzhou, China, Post Code: 510725) //Journal of Engineering for Thermal Energy & Power. -2016, 31(11). -55 ~ 58

On the basis of various H_2O and CO_2 molar ratios and total blackness at various temperature and travelling distances calculated by using a narrow band model, proposed was a new weighted sum of grey gases model correlation formula for calculating the heat quantity exchanged in radiation from gases under the condition of oxygen-enriched combustion. In the above-mentioned correlation formula, both grey gas absorption coefficient and the weighted value are a function of the gas temperature and the molar ratio between the H_2O and CO_2, however, in the traditional grey gas weight sum model, the grey gas absorption coefficient is a constant. The new correlation formula can enhance the accuracy of the grey gas weight sum model and compared with the total blackness obtained by using the statistical narrow band model, the maximal relative error is within 5%. **Key words:** narrow band model, grey gas weight sum, correlation formula, molar ratio, temperature

燃煤飞灰碳质颗粒与水相互作用的模拟研究 = Study of the Simulation of the Interaction Between Water and Carbon-contained Particles in Flying Ash Produced in Combustion of Coal [刊,汉] /LV Hai-hua, GUO Xin (National Key Laboratory on Coal Combustion, Central China University of Science and Technology, Wuhan, China, Post Code: 430074) //Journal of Engineering for Thermal Energy & Power. -2016, 31(11). -59 ~ 63

A model for the microporous amorphous carbon atomic configuration was established by using the molecular dynamics melting-quenching method and the adsorption of water-steam in the model was investigated. A model for carbon-contained particles at various initial densities was built and the radial distribution function and pore diameter distribution curves of the carbon-contained particles were calculated respectively. In the meantime, the isotherm of the carbon-contained particles to adsorb water molecules at various initial densities was studied and the influence of the temperature on the carbon-contained particles at a single initial density to adsorb water molecules was also investigated. It has been found that for amorphous carbon-contained particles having a same number of atoms, the greater the initial density, the smaller the probability of a relatively big pore diameter will emerge inside. With an increase of the initial density, the number of water molecules adsorbed by the carbon-contained particles will gradually decrease. At the same time, with an increase of temperature, the number of water molecules adsorbed by the carbon-contained particles will continuously decrease. **Key words:** pulverized coal, molecular dynamics, grand canonical